Metabolism 158 (2024) 155952

Contents lists available at ScienceDirect

Metabolism

journal homepage: www.journals.elsevier.com/metabolism

The lipopolysaccharide-TLR4 axis regulates hepatic glutaminase 1 expression promoting liver ammonia build-up as steatotic liver disease progresses to steatohepatitis

Maria Mercado-Gómez [a], Naroa Goikoetxea-Usandizaga [a,b], Annarein J.C. Kerbert [c], Leire Uraga Gracianteparaluceta [d], Marina Serrano-Maciá [a], Sofia Lachiondo-Ortega [a], Rubén Rodriguez-Agudo [a], Clàudia Gil-Pitarch [a], Jorge Simón [a,b], Irene González-Recio [a], Marcos F. Fondevila [e], Pablo Santamarina-Ojeda [f,g,h], Mario F. Fraga [f,g,h,i], Rubén Nogueiras [e,j,k], Javier de las Heras [d,l,m], Rajiv Jalan [c], María Luz Martínez-Chantar [a,b,*], Teresa C. Delgado [a,d,n,**]

[a] *Liver Disease Laboratory, Center for Cooperative Research in Biosciences (CIC bioGUNE), Basque Research and Technology Alliance (BRTA), 48160 Derio, Bizkaia, Spain*
[b] *Centro de Investigación Biomédica en Red de Enfermedades Hepáticas y Digestivas (CIBERehd), 28029 Madrid, Spain*
[c] *Liver Failure Group, Institute for Liver and Digestive Health, University College London, Royal Free Campus, London, United Kingdom*
[d] *Biobizkaia Health Research Institute, 48903 Barakaldo, Spain*
[e] *Department of Physiology, CIMUS, University of Santiago de Compostela-Instituto de Investigación Sanitaria, 15782 Santiago de Compostela, Spain*
[f] *Health Research Institute of the Principality of Asturias (ISPA), 33011 Oviedo, Asturias, Spain*
[g] *Spanish Biomedical Research Network in Rare Diseases (CIBERER), 28029 Madrid, Spain*
[h] *Nanomaterials and Nanotechnology Research Center (CINN), Spanish National Research Council (CSIC), 33940 El Entrego, Asturias, Spain*
[i] *Institute of Oncology of Asturias (IUOPA), University of Oviedo, 33006 Oviedo, Asturias, Spain*
[j] *CIBER Fisiopatologia de la Obesidad y Nutrición (CIBERobn), 28029 Madrid, Spain*
[k] *Galician Agency of Innovation (GAIN), Xunta de Galicia, Santiago de Compostela, Spain*
[l] *Division of Paediatric Metabolism, CIBERER, MetabERN, Cruces University Hospital, 48903 Barakaldo, Spain.*
[m] *Department of Paediatrics, University of the Basque Country (UPV/EHU), 48940 Leioa, Spain*
[n] *IKERBASQUE, Basque Foundation for Science, Bilbao, Spain*

ARTICLE INFO

Keywords:
Ammonia
Glutaminase
Urea cycle
Toll-like receptor 4
Lipopolysaccharide
Metabolic-associated steatotic liver disease

ABSTRACT

Introduction: Ammonia is a pathogenic factor implicated in the progression of metabolic-associated steatotic liver disease (MASLD). The contribution of the glutaminase 1 (GLS) isoform, an enzyme converting glutamine to glutamate and ammonia, to hepatic ammonia build-up and the mechanisms underlying its upregulation in metabolic-associated steatohepatitis (MASH) remain elusive.

Methods: Multiplex transcriptomics and targeted metabolomics analysis of liver biopsies in dietary mouse models representing the whole spectra of MASLD were carried out to characterize the relevance of hepatic GLS during disease pathological progression. In addition, the acute effect of liver-specific GLS inhibition in hepatic ammonia content was evaluated in cultured hepatocytes and in *in vivo* mouse models of diet-induced MASLD. Finally, the regulatory mechanisms of hepatic GLS overexpression related to the lipopolysaccharide (LPS)/Toll-like receptor 4 (TLR4) axis were explored in the context of MASH.

Results: In mouse models of diet-induced MASLD, we found that augmented liver GLS expression is closely associated with the build-up of hepatic ammonia as the disease progresses from steatosis to steatohepatitis. Importantly, the acute silencing/pharmacological inhibition of GLS diminishes the ammonia burden in cultured primary mouse hepatocytes undergoing dedifferentiation, in steatotic hepatocytes, and in a mouse model of diet-induced steatohepatitis, irrespective of changes in ureagenesis and gut permeability. Under these conditions, GLS upregulation in the liver correlates positively with the hepatic expression of TLR4 that recognizes LPS. In

* Correspondence to: M. L. Martínez-Chantar, CIC bioGUNE, Ed. 801A Parque Tecnológico de Bizkaia, 48160 Derio, Bizkaia, Spain.
** Correspondence to: T. C. Delgado, Biobizkaia Health Research Institute, Biocruces Bizkaia edificio 1, Pza. Cruces S/N, 48903 Barakaldo, Bizkaia, Spain.
E-mail addresses: mlmartinez@cicbiogune.es (M.L. Martínez-Chantar), tcardosodelgado@gmail.com (T.C. Delgado).

https://doi.org/10.1016/j.metabol.2024.155952
Received 22 February 2024; Accepted 7 June 2024
Available online 19 June 2024

agreement, the pharmacological inhibition of TLR4 reduces GLS and hepatic ammonia content in LPS-stimulated mouse hepatocytes and hyperammonemia animal models of endotoxemia.
Conclusions: Overall, our results suggest that the LPS/TLR4 axis regulates hepatic GLS expression promoting liver ammonia build-up as steatotic liver disease progresses to steatohepatitis.

1. Introduction

Ammonia homeostasis is a dynamic process, adapting the physiological response to nutrients, hormones, and metabolites, but also under pathological conditions [1,2]. Whereas controlled levels of endogenous ammonia provide a gut-brain signaling basis for emotional behavior [3], elevated blood ammonia, hyperammonemia, is a common complication of a wide variety of both inherited and acquired hepatic diseases (e.g., urea cycle disorders, liver failure, and cirrhosis) [4–8]. Recently, our group and others described the build-up of hepatic ammonia as a hallmark of metabolic-associated steatohepatitis (MASH), a more severe stage within the metabolic-associated steatotic liver disease (MASLD) spectrum [9,10].

Whole-body ammonia balance is a tightly regulated process where the gut-liver axis is central. Indeed, the overproduction of ammonia by gut microbiota, synergistically interacting with ethanol, is a significant contributor to alcohol-associated liver disease [11]. Although patients with MASLD are characterized by an enrichment of gut ammonia-producing bacteria [12,13], the direct contribution of gut-derived ammonia to the accumulation of hepatic ammonia underlying MASH or its indirect effects by facilitating toxic molecule drainage through disrupted gut permeability has not been demonstrated. Otherwise, the changes in hepatic metabolic processes regulating ammonia homeostasis have been further explored. On this basis, the accumulation of hepatic ammonia in patients and animal models of MASH with significant fibrosis is associated with a reduction in gene, protein expression, and activity of urea cycle enzymes (UCEs), a group of enzymes involved in ammonia detoxification [10]. In addition, our group and others demonstrated that the expression of the high-activity glutaminase 1 isoenzyme (GLS) is augmented both in steatotic hepatocytes and in activated hepatic stellate cells, the main fibrogenic cell type, and liver biopsies of MASH patients [14,15]. Treatment with the ammonia scavenger ornithine phenylacetate prevents hepatocyte cell death and significantly reduces inflammation and fibrosis in liver slices from MASH patients and in mouse models of this disease [16,17]. Also, treatment with another ammonia scavenger, the L-ornithine L-aspartate, reduces ammonia release and normalizes metabolic parameters in models of steatosis [18]. Likewise, the sustained specific silencing/inhibition of hepatic GLS ameliorates liver steatosis and inflammation in mouse models of MASH [14,19]. Nonetheless, the contribution of hepatic GLS expression or its therapeutic reduction to the modulation of hepatic ammonia in steatohepatitis remains to be explored.

Herein, we provide compelling evidence that increased hepatic GLS is associated with the build-up of hepatic ammonia in pre-clinical mouse models of MASLD. In addition, we have shown that stimulation with LPS, a natural TLR4 ligand, induces hepatic GLS expression in isolated mouse hepatocytes. On the contrary, GLS overexpression is hampered by TLR4 pharmacological inhibition both in LPS-stimulated hepatocytes and in hyperammonemia animal models of endotoxemia and Acute on Chronic Liver Failure (ACLF). Overall, our results suggest that augmented signaling through the LPS/TLR4 axis induces hepatic GLS overexpression in the liver, a process most probably mediated by NF-κB activation, contributing to hepatic ammonia build-up underlying steatohepatitis. Deciphering the upstream regulators of GLS and its regulatory mechanisms will shed light on the triggering mechanisms driving the progression of MASLD.

2. Methods

2.1. Animal models

All animal experiments were performed according to the ARRIVE guidelines under the guidelines of the European Research Council for animal care after approval by the Institutional Animal Welfare and Ethics Committee.

2.1.1. Diet-induced MASLD

Three-month-old male C57BL/6J rodents were acquired from Charles River (St Germain sur l'Arbresle, France) and maintained on a 12/12 h light/dark cycle at 21 ± 1 °C and humidity of 45 ± 10 %. Mice were maintained with ad libitum access to water and different diet interventions (Research Diets Inc., New Jersey, USA): high-fat diet (HFD) (D12451) with 45 % kcal from fat, choline-deficient high-fat diet (CDHFD) (D05010402), a diet devoid of choline with 0.1 % methionine, amino acid-defined diet (CDAA) (A02082006i) and finally a diet devoid of choline with 0.1 % methionine and high fat-enriched (CDAHFD) (A06071302). A control group was fed a regular diet containing 1.030 mg/kg choline, 0.3 % methionine, and 13 % kcal from fat (Teklad Global). Another group of animals of 3-month-old male C57BL/6J rodents was maintained for 16 weeks on CDHFD. In another experiment, after 6 weeks of CDAHFD, 3-month-old male C57BL/6J mice were randomly separated into two experimental groups and tail-vein injected either with a single injection of 150 μL of 27 mM pre-designed *Gls*-specific siRNA (Custom Ambion In vivo siRNA by Life technologies- 5′-3′-GGGCAACAGUGUUAAGGGAtt, 3′-5′-UCCCUUAACACUGUUGCCCat) or control siRNA (Custom Ambion In vivo siRNA by Life technologies) with Invivofectamine 3.0 Reagent (Thermo Fisher Scientific) as transfection reagent prepared, according to the manufacturer's recommendation. At the beginning of the dietary intervention, submandibular blood was collected.

2.1.2. Endotoxemia and hyperammonemia

Another group of male 3-month-old C57BL/6J mice were given an amino acid (AA)-enriched diet by adding an AA mixture to a standard powdered diet in a 1:2 ratio for 14 days. This AA diet mixture was developed as an ammoniagenic diet and can be found in Supplemental Table 1 [20,21]. Mice fed an AA diet were treated with either the TLR4 antagonist TAK-242 (Takeda, JP; Akaza, UK) or vehicle (captisol). In addition, treatment naïve male $Tlr4^{-/-}$ mice were studied (The Jackson Laboratory, B6. B10ScN-*Tlr4*$^{lps\text{-}del}$/JthJ, stock number 007227). Finally, a rat model of Acute-on-Chronic Liver Failure (ACLF) was studied [22]. Briefly, Sprague Dawley rats (260 ± 20 g, age 8–10 weeks) were studied 4 weeks after sham or bile duct ligation (BDL) surgery. ACLF was induced by the i.p. injection of 0.025 mg/kg LPS (*Klebsiella pneumonia*, Sigma, UK). TAK-242 (10 mg/kg i.p.) or vehicle (captisol) was administered prophylactically 3 h before the LPS injection and animals were sacrificed 3 h after the LPS injection.

2.2. Primary mouse hepatocytes

Primary mouse hepatocytes were obtained through collagenase liver perfusion of male adult C57BL/6J male mice as previously described [14]. Upon attachment, primary hepatocytes were maintained in MEM media (GIBCO). Alternatively, some experimental groups were incubated with methionine and choline-deficient DMEM/F-12 media (GIBCO). The following treatments were given to cells: 10 ng/mL

lipopolysaccharide (LPS) (Sigma-Aldrich, St. QuentilFallavier, France), 200 nM TAK-242 (Sigma-Aldrich, Sigma-Aldrich, St. QuentilFallavier, France) and 10 μM Bis-2(5-phenylacetamido-1,3,4-thiadiazol-2-yl)ethyl sulfide (BPTES) (Sigma-Aldrich, St. QuentilFallavier, France). In some experiments, isolated mouse primary hepatocytes were transfected with 100 nM *Gls* siRNA- GCAAUAGGAUAUUACUUAAtt, UUAA-GUAAUAUCCUAUUGCtt or unrelated siRNA(QIAGEN, Spain) using DharmaFECT 1 reagent (Dharmacon). Controls were transfected with an unrelated siRNA (QIAGEN, Madrid, Spain).

Detailed information on the methods and statistical analysis in the Supplemental Material.

3. Results

3.1. Disrupted liver nitrogen metabolism in pre-clinical mouse models of diet-induced MASLD

Pre-clinical animal models of MASLD are useful for unraveling undetected events involved in the pathology of the disease. We have carried out multiplex transcriptional hepatic profiling of mice maintained for 6 weeks on a control diet, high-fat diet (HFD), choline-deficient high-fat diet (CDHFD), choline-deficient L-amino acid-defined diet (CDAA) and choline-deficient L-amino acid-defined high-fat diet (CDAHFD), representing different stages of the MASLD pathophysiology classified according to a histological scoring system adapted for rodents [23] (Suppl. Fig. 1a,b and Suppl. Table 2). As previously observed, animals on CDAA and CDAHFD for 6 weeks are characterized by significant mild fibrosis [24]. Volcano plots representing the differentially expressed hepatic genes in each experimental group of diet-induced MASLD plotted against the control diet group are shown in Fig. 1a. Overall, an increase in the expression of methionine adenosyltransferase 2 A (*Mat2A*) is observed in all MASLD mouse models. In the more advanced models of the disease, characterized by aberrant steatosis and inflammation together with liver fibrosis, the following changes were detected: increased platelet glycoprotein 4 (*Cd36*) involved in fatty acid uptake, CD63 antigen related to extracellular vesicles secretion, hexosaminidase A accounting for lysosomal activity, B cell leukemia/lymphoma related protein A1a associated to apoptosis, chemokine (C—C motif) ligand 2 (*CCl2*), increased collagen, type VI, alpha 2 and collagen, type IV, alpha 1. A heatmap showing the metabolic signatures and pathway score changes across liver tissues of the different mouse models of diet-induced MASLD that were explored is described in Fig. 1b. As expected, samples from each dietary intervention corresponding to differential stages of the MASLD pathological spectrum tend to cluster, indicating that they present more similar pathway score profiles. Importantly, pathways related to deregulated liver nitrogen metabolism, including arginine and glutamine metabolism, are overrepresented in the two groups of animals with overt steatohepatitis and significant liver fibrosis, animals on a 6-week CDAA and CDAHFD. In addition, pathways most strongly associated with prominent signals in the heatmap include gene sets related to lysosomal degradation (PC1 = 0.92), Toll-like receptor (TLR) signaling (PC1 = 0.86), Keap/NRF2 pathway (PC1 = 0.81), fatty acid synthesis (PC1 = 0.75) and antigen presentation (PC1 = 0.75).

3.2. Accumulation of hepatic ammonia and disrupted urea cycle in pre-clinical mouse models of diet-induced MASLD

Ammonia, one of the most important nitrogen-containing compounds, is significantly increased in the livers of mouse models of diet-induced steatohepatitis with or without significant fibrosis: animals on CDHFD, CDAA, and CDAHFD for 6 weeks, respectively (Fig. 2a). Of relevance, both in CDHFD and CDAHFD-fed animals, blood hyperammonemia is detected after 6 weeks of CDAHFD pinpointing that hepatic ammonia accumulation precedes blood hyperammonemia in MASLD natural history progression (Suppl. Fig. 2a,b), agreeing with earlier clinical findings [10].

The urea cycle is the main pathway that accounts for liver ammonia detoxification. Reduced gene expression of the urea cycle enzymes (UCEs), carbamoyl phosphate synthetase 1 (*Cps1*), ornithine transcarbamoylase (*Otc*), argininosuccinate synthetase 1 (*Ass1*), argininosuccinate lyase (*Asl*) and arginase 1 (*Arg1*) was observed in mouse models of diet-induced MASH and fibrosis (animals maintained on CDAA and CDAHFD for 6 weeks). Hepatic *Ass1* is further downregulated in early animal models of MASLD (animals maintained on HFD and CDHFD for 6 weeks) (Fig. 2b). Reduced expression of hepatic UCEs is associated with higher hepatic levels of the urea cycle intermediates ornithine and arginine. Besides being a metabolic intermediary in the urea cycle, ornithine is also a substrate for polyamine synthesis in eukaryotes. Indeed, ornithine decarboxylation by ornithine decarboxylase leads to the first polyamine, putrescine. Spermidine and spermine are then synthesized from putrescine. Hepatic putrescine levels are increased in animals fed for 6 weeks on a CDAHFD diet agreeing with earlier evidence [25]. Unlike putrescine, hepatic spermine levels are not altered in mice on CDAHFD for 6 weeks. A key step in the polyamine biosynthetic pathway is catalyzed by S-adenosylmethionine decarboxylase, using S-adenosyl-L-methionine (SAMe), the major methyl donor in cells. As previously observed, a reduction in the hepatic SAMe and S-adenosylhomocysteine (SAH) ratio is observed in all the mouse models of diet-induced MASLD studied [26]. Finally, another well-established methyl donor, betaine, is also reduced in all the animal models of diet-induced MASLD studied (Fig. 2c), which agrees with earlier evidence showing that this condition is associated with a state of betaine insufficiency [27].

Overall, accumulation of hepatic ammonia is a hallmark of steatohepatitis, and reduced ureagenesis through the urea cycle is a hallmark of mouse models of steatohepatitis with significant liver fibrosis.

3.3. Rewiring of liver glutamine metabolism in pre-clinical mouse models of diet-induced MASLD

Previous evidence has shown that the serum glutamate/glutamine ratio correlates with fibrosis severity in MASLD patients and mouse models [28]. Here, we found that hepatic glutamine concentrations are not altered as the disease progresses from steatosis to MASH, somehow expected considering the overall high abundance of this amino acid in the whole body. Conversely, hepatic glutamate is significantly augmented in animal models fed with CDHFD, CDAA, and CDAHFD for 6 weeks (Fig. 3a). Within the liver, glutamine is synthesized from glutamate through glutamine synthetase (Glul), the expression of which is significantly reduced at the protein level in animals maintained for 6 weeks on CDAHFD. Alternatively, the mitochondrial enzyme glutaminase can convert hepatic glutamine to glutamate and ammonia. The glutaminase family consists of two isoenzymes, the GLS and the GLS2 genes. Under healthy conditions, GLS2 is the predominant isoenzyme in the liver whereas GLS is mostly expressed in the kidney and spleen. Both early and advanced mouse models of diet-induced MASLD (CDHFD, CDAA, and CDAHFD for 6 weeks) are characterized by increased hepatic expression of the high activity isoform Gls while a reduction of hepatic Gls2 is observed (Fig. 3b,c), in agreement with early evidence [14].

To confirm that increased Gls hepatic expression is a hallmark in more chronic obesogenic mouse models, we fed rodents with CDHFD for longer periods. After 16 weeks of CDHFD, mice are obese and characterized by augmented body weight (Fig. 4a), and hepatic steatosis with elevation of liver inflammation and distribution of collagen fibers in the liver parenchyma (Suppl. Fig. 3a). Also, serum transaminases and cholesterol are augmented (Suppl. Table 3). Under these conditions, hepatic Gls expression at the mRNA and protein levels is increased whereas glutamine synthetase, Gls2 together with the expression of UCEs remains unaltered (Fig. 4b-d). After 16 weeks of CDHFD, hepatic ammonia is significantly increased, as measured by both Nessler histological staining and biochemical assay (Fig. 4e,f). In agreement, patients diagnosed with steatohepatitis are also characterized by increased

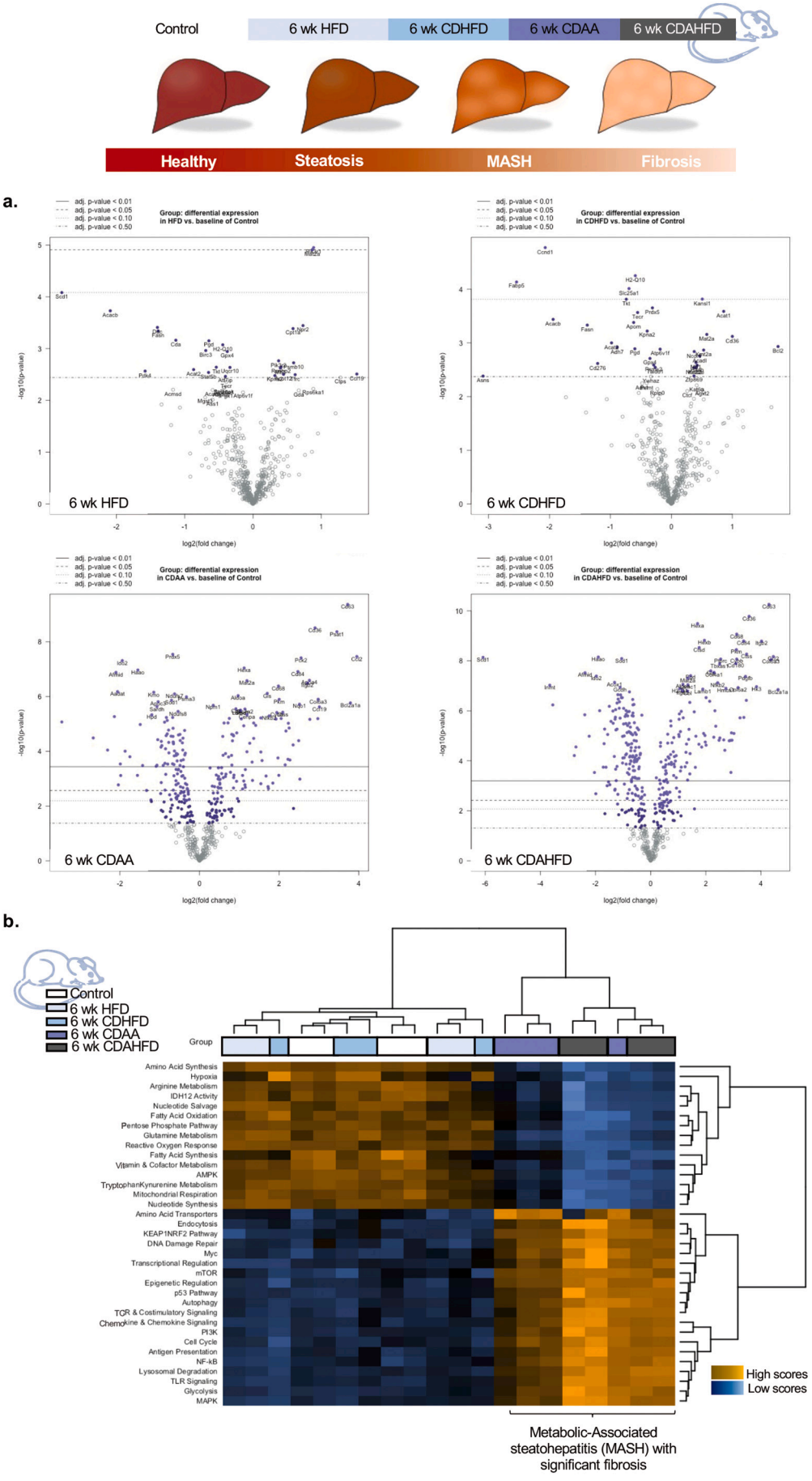

(caption on next page)

Fig. 1. Multiplex transcriptomic profiling in pre-clinical models of diet-induced metabolic-associated steatotic liver disease (MASLD). a. Volcano plot representation of the differential genes assessed by multiplex transcriptomic profiling expressed in pre-clinical models of experimental MASLD relative to control. b. Heatmap with metabolic signatures and pathway score changes. Mice were maintained for 6 weeks either on high-fat diet (HFD), choline-deficient high-fat diet (CDHFD), choline-deficient L-amino acid-defined diet (CDAA), and choline-deficient L-amino acid-defined high-fat diet (CDAHFD) and compared to standard rodent chow diet (Control). $N = 4$ rodents were used for each experimental group. Analysis was performed using nSolver® analysis package as detailed in the Supplemental material.

hepatic Gls (Fig. 4g) according to the data available [29].

In summary, our results confirm that hepatic GLS overexpression is increased in steatohepatitis irrespective of changes in other glutamine metabolism intermediates or UCEs expression.

3.4. Specific silencing or pharmacological inhibition of glutaminase 1 (GLS) hampers hepatocyte intracellular ammonia build-up

Primary mouse hepatocytes were initially used to investigate if the specific modulation of hepatocyte GLS controls intracellular ammonia accumulation. It has been widely described in the literature that isolated primary hepatocytes in 2D cultures undergo dedifferentiation. Indeed, hepatocytes undergoing dedifferentiation present loss of hepatocyte nuclear factor 4 (HNF4), a central regulator of hepatocyte dedifferentiation, and decreased expression of CYP genes (*Cyp1a2, Cyp7a1*) (Suppl. Fig. 4a,b), as seen in earlier reports [30]. Importantly, dedifferentiated mouse hepatocytes show increased expression of Gls and unaltered *Gls2* expression, whilst UCE expression is decreased (Fig. 5a-c), partially mimicking our previous observations in mouse models of diet-induced steatohepatitis. Under these conditions, intracellular hepatic ammonia increases (Fig. 5d). Therefore, we decided to specifically silence Gls in isolated primary mouse hepatocytes undergoing dedifferentiation. Hepatocyte Gls silencing by using molecular approaches was not associated either with changes in the expression of *Gls2* or altered gene expression of UCEs. Furthermore, dedifferentiation markers were not altered as a result of Gls silencing (Suppl. Fig. 4c,d). Although no changes were detected either in *Gls2*, glutamine synthetase, or UCE mRNA expression, intracellular ammonia content is significantly reduced after *Gls* silencing (Fig. 5d). Finally, we inhibited Gls by using a small specific pharmacological inhibitor, BPTES, in primary mouse hepatocytes incubated with a cell media deficient in methionine and choline (MCD), which leads to the accumulation of intracellular lipids. Cell hepatocyte lipid content is reduced upon pharmacological inhibition of GLS with BPTES, confirming earlier evidence from our group [14]. Noteworthy, treatment with BPTES, both to hepatocytes incubated with control media or with MCD media, significantly reduces intracellular ammonia content (Fig. 5e,f).

Overall, we have shown that the specific inhibition of GLS in isolated mouse hepatocytes is associated with a reduction in lipid content and accounts for reduced intracellular ammonia build-up.

3.5. Acute silencing of hepatic glutaminase 1 (GLS) diminishes hepatic ammonia build-up in a pre-clinical mouse model of diet-induced steatohepatitis

To further assess the role of deregulated hepatic GLS activity in hepatic ammonia accumulation, we acutely silenced hepatic Gls using invivofectamine and siRNA administered by tail vein injection at 48 h before sacrifice to animals kept on CDAHFD for 6 weeks. Specific acute silencing of hepatic Gls in mouse livers was confirmed by mRNA and Western blot analysis, with a concomitant decrease in liver tissue glutaminase activity (Fig. 6a-c). On the contrary, the acute silencing of hepatic Gls in CDAHFD-fed rodents does not account for altered Gls2 expression and distribution (Fig. 6b,d). Likewise, the specific silencing of hepatic Gls does not alter the overall distribution of glutamine synthetase (Glul) within the liver parenchyma (Fig. 6d) and was not associated with significant modulation of the expression and activity of UCEs (Fig. 6e). Contrary to what our group has previously shown with chronic hepatic Gls silencing in related mouse models of MASLD [14], acute hepatic Gls silencing was not sufficient to reverse liver steatosis and did not alter serum biochemistry parameters. Even though the inflammation marker F4/80 is not altered, as assessed by IHC staining, mRNA levels of some inflammatory markers (*Tnf, Il6, Il10, Il1b, Nrf2,* and *iNos)* are tendentially decreased upon acute hepatic GLS silencing. Toll-like receptor 4 (TLR4), a receptor with a central role in innate immune signaling orchestrating inflammatory responses, is also augmented after 6 weeks of CDHFD, but only tendentially decreased after acute silencing of hepatic Gls. Finally, liver fibrosis, assessed by Sirius red staining and the hydroxyproline kit is mildly reduced after Gls acute silencing (Suppl. Fig. 5a-c, Suppl. Table 4).

Disrupted gut integrity is implicated in ammonia homeostasis. Immunohistochemical analysis of the intracellular scaffold protein zonula occludens (ZO)-1, a good marker for tight junction integrity in the intestinal barrier affecting intestinal permeability, shows that in controls there is strong labeling of enterocyte cytoplasm covering the tip with a progressive decrease towards the bases of villi. In contrast, moderate labeling of enterocyte cytoplasm is observed in the duodenal mucosa of CDAHFD-fed animals. Disrupted gut integrity is not significantly altered after acute hepatic Gls silencing for 48 h. Furthermore, an assay to indirectly measure intestinal permeability shows that a leaky gut is a hallmark of CDAHFD animals, a feature that is not significantly altered after hepatic Gls silencing. In agreement with disrupted intestinal permeability, serum LPS content is augmented in the CDAHFD compared with healthy control animals, which remains unaltered after hepatic Gls silencing (Fig. 6f-h).

Finally, the acute hepatic Gls silencing in animal models fed a CDAHFD for 6 weeks significantly reduces hepatic ammonia content, as assessed using Nessler staining analysis and biochemical assay (Fig. 6i,j). Taken together, our results show that hepatic GLS expression plays an important role in controlling hepatic ammonia accumulation underlying steatohepatitis.

3.6. Glutaminase 1 (GLS) promoter methylation is not altered in an early pre-clinical mouse model of diet-induced steatohepatitis

To date, the mechanisms underlying GLS regulation in steatohepatitis remain elusive. Increasing evidence indicates that many chronic diseases, including MASLD, are affected by aberrant DNA methylation [31] in response to environmental factors, including diet and gut bacterial toxins [32,33]. DNA methylation has a specific effect on gene expression: hypermethylation of the CpG islands in the promoter region of genes is associated with gene repression, and hypomethylation of the global DNA affects genomic stability and integrity [34]. Analysis of the publicly available cancer TCGA OMICS data [35,36] shows that GLS expression at mRNA level is increased in a series of cancers related to the gastrointestinal system, including liver hepatocellular carcinoma (HCC) (Suppl. Fig. 6a). Importantly, in the case of HCC, GLS gene hypomethylation is a frequent epigenetic event that correlates positively with the increased expression of GLS, depending on the tumoral grade (Suppl. Fig. 6b,c). Therefore, we decided to evaluate the degree of Gls promoter methylation in liver biopsies of mouse models of MASLD. In general, the liver Gls promoter is hypomethylated in the mouse liver. Animals on CDHFD and CDAA for 6 weeks, characterized by increased liver Gls expression, do not present alterations of the Gls promoter methylation compared with healthy control animals. Otherwise, Gls promoter methylation is significantly reduced in the most advanced mouse model of steatohepatitis, animals on CDAHFD for 6 weeks (Suppl. Fig. 6d). Thus, even though the epigenetically mediated GLS promoter

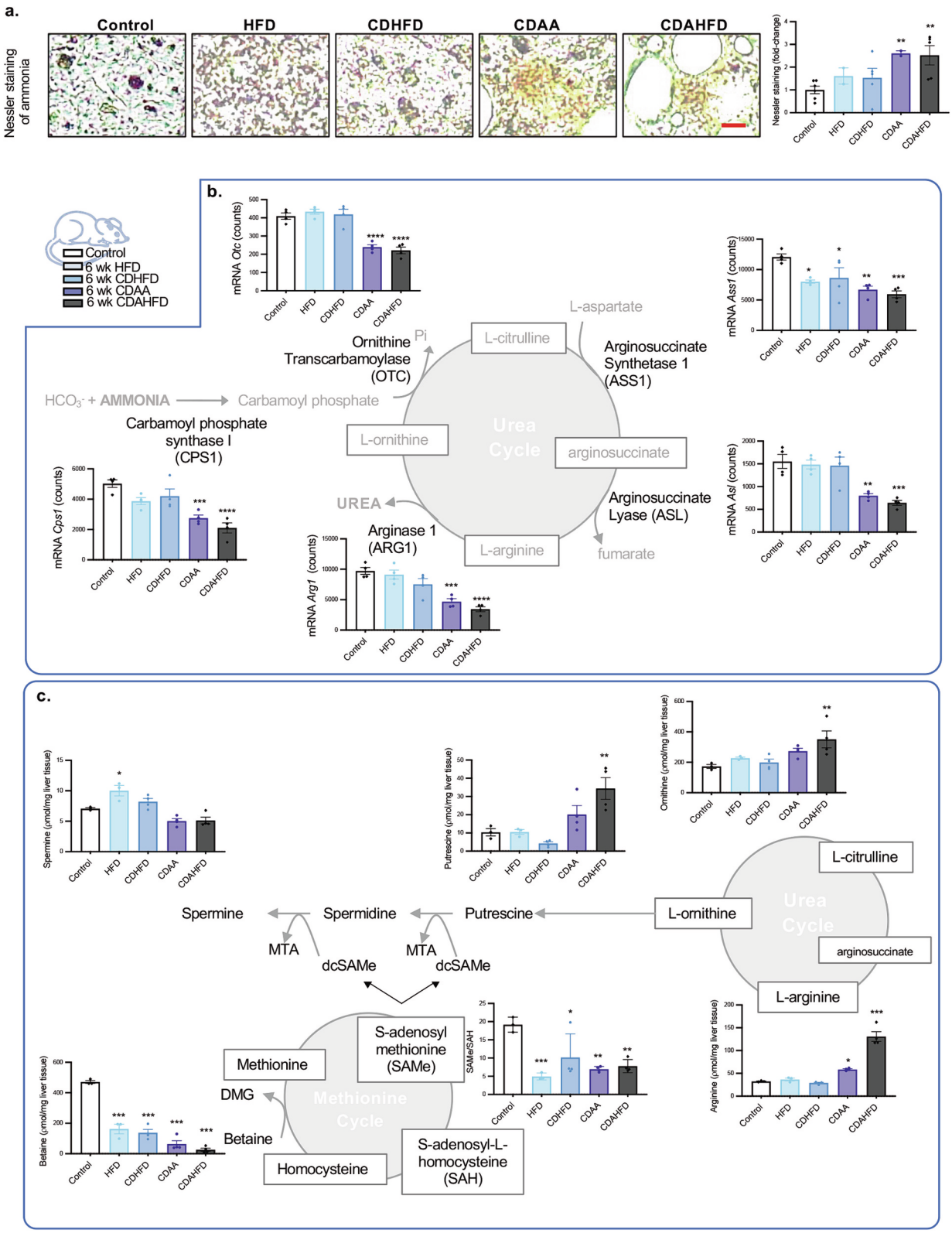

Fig. 2. Accumulation of hepatic ammonia and disrupted urea cycle in pre-clinical mouse models of diet-induced metabolic-associated steatotic liver disease (MASLD). a. Hepatic ammonia content assessed by Nessler histological staining; b. Transcriptomic analysis of urea cycle enzymes (UCEs) and; c. hepatic nitrogen metabolism-related metabolites in animal models of diet-induced MASLD. Mice were maintained for 6 weeks on a high-fat diet (HFD), choline-deficient high-fat diet (CDHFD), choline-deficient L-amino acid-defined diet (CDAA), and choline-deficient L-amino acid-defined high-fat diet (CDAHFD) and compared to standard rodent chow diet (Control). Data in columns are represented as average ± SEM. A $p < 0.05$ was considered statistically significant after a one-way ANOVA test and post-hoc Tukey's test compared to the control group. *$p < 0.05$, **$p < 0.01$, ***$p < 0.001$ and ****$p < 0.0001$ relative to the control group are shown. At least N = 4 rodents were used for each experimental group. The red scale bar corresponds to 500 μm. (For interpretation of the references to colour in this figure legend, the reader is referred to the web version of this article.)

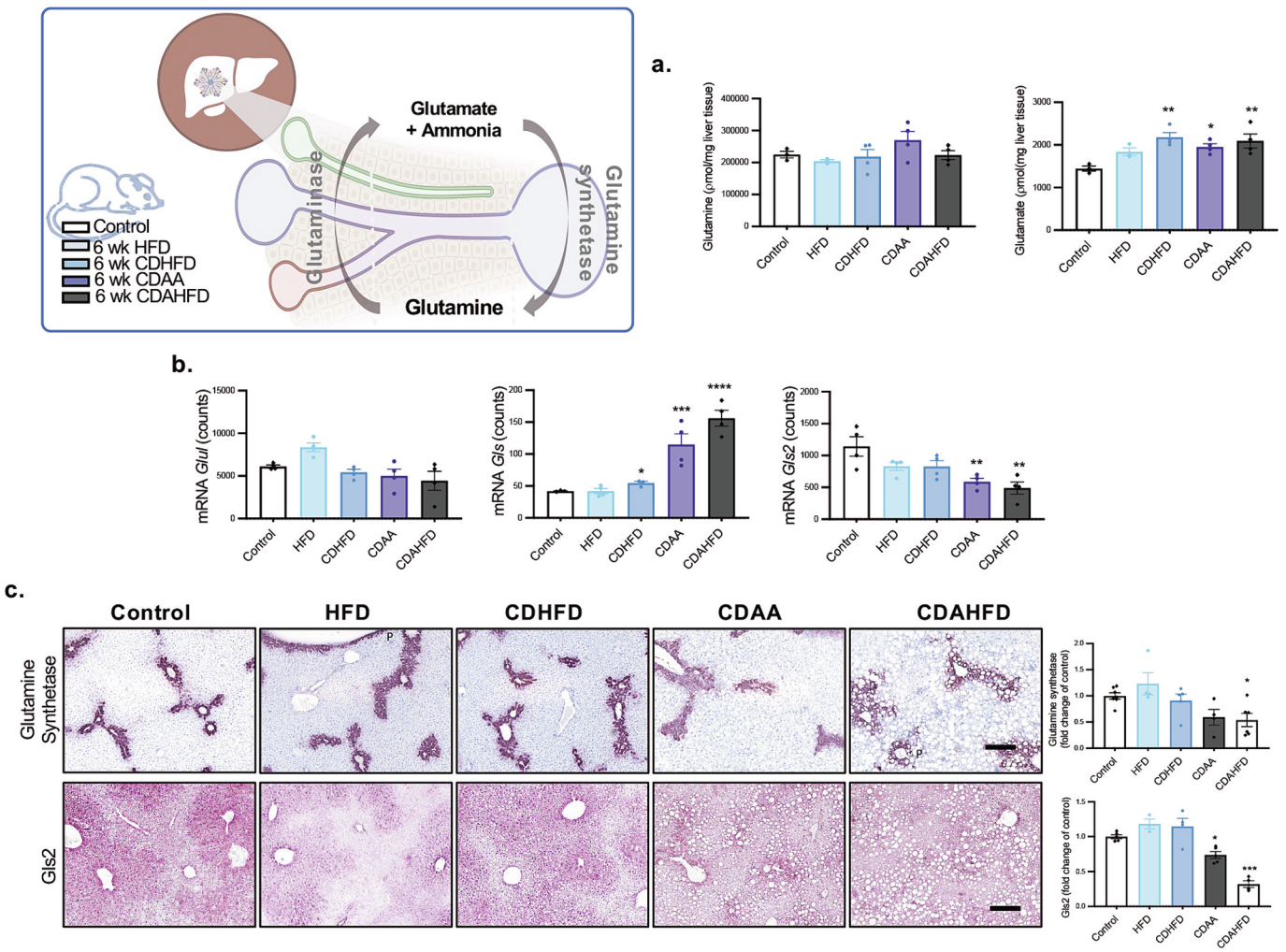

Fig. 3. Rewiring of liver glutamine metabolism in pre-clinical mouse models of diet-induced steatohepatitis. a. Liver glutamine and glutamate concentration; b. Transcriptomic analysis of liver glutamine-related metabolism and c. Liver glutamine-related metabolism enzymes protein expression by immunohistochemical staining in animal models of diet-induced metabolic-associated steatotic liver disease (MASLD). Mice were maintained for 6 weeks on a high-fat diet (HFD), choline-deficient high-fat diet (CDHFD), choline-deficient L-amino acid-defined diet (CDAA) and choline-deficient L-amino acid-defined high-fat diet (CDAHFD) and compared to standard rodent chow diet (Control). Data in columns are represented as average ± SEM. A $p < 0.05$ was considered statistically significant after a one-way ANOVA test and post-hoc Tukey's test compared to the control group. *$p < 0.05$, **$p < 0.01$, ***$p < 0.001$ and ****$p < 0.0001$ relative to the control group are shown. At least N = 4 rodents were used for each experimental group. Abbreviations: *Glul*. Glutamine synthase, *Gls*. Glutaminase, *Gls2*. Glutaminase 2. The black scale bar corresponds to 100 µm. Created with BioRender.com.

methylation is relevant in advanced steatohepatitis, other regulatory mechanisms appear to be involved in triggering GLS upregulation in early MASH.

3.7. Toll-like receptor 4 (TLR4), an upstream regulator of hepatic glutaminase 1 (GLS)

Metabolic endotoxemia, the chronic elevation of serum LPS levels, is a hallmark of MASH [37,38]. More specifically, Toll-like receptor 4 (TLR4), the key receptor involved in LPS signaling, is overexpressed in MASH patients [39]. Our multiplex transcriptomic analysis of the different animal models of MASLD highlighted that gene sets related to TLR signaling are variables strongly associated with the onset of steatohepatitis. In agreement, the hepatic mRNA expression of *Tlr4* shows a strong positive correlation with *Gls* in liver biopsies of animal models of diet-induced MASLD (Fig. 7a). Likewise, mouse primary hepatocytes undergoing dedifferentiation, a process where Gls is overrepresented, are characterized by increased *Tlr4* mRNA expression (Fig. 7b). In light of these results, we have further observed that stimulation of isolated mouse hepatocytes with LPS induces the expression of cellular Gls in association with increases in the expression of *Tlr4* and inflammatory markers (*Tnf* and *Il6*). Under these conditions, pre-treatment with TAK-242, a selective TLR4 inhibitor, diminished *Tlr4* levels and hampered LPS-induced hepatocyte Gls upregulation (Fig. 7c,d). Of relevance, LPS-induced modulation of Gls is associated with increased cellular ammonia content, which is reduced upon pre-treatment either with TAK-242 or the specific GLS pharmacological inhibitor, BPTES (Fig. 7e, f). In agreement with our in vitro results, *Tlr4*$^{-/-}$ mice present basally lower levels of hepatic Gls and tendentially reduced hepatic ammonia content (Suppl. Fig. 7a,b).

TAK-242 binds selectively to TLR4 and is a signaling inhibitor from the intracellular domain of TLR4. TAK-242 can disrupt the interaction of TLR4 with adapter molecules, thereby inhibiting TLR4 signal transduction and its downstream signaling events. Thus, we have evaluated the effects of TLR4 inhibition using TAK-242 in 2 models of hyperammonemia and endotoxemia: *i)* mice on an AA-enriched diet for 14 days and *ii)* rats with BDL-induced liver cirrhosis and superimposed endotoxemia by LPS injection, a model of Acute on Chronic Liver Failure (ACLF). Mice on an AA-enriched diet show increased weight loss relative to animals on a control diet (Ctrl = 1.0 ± 0.4 vs. AA-diet = 5.3 ± 0.8 g, *p*

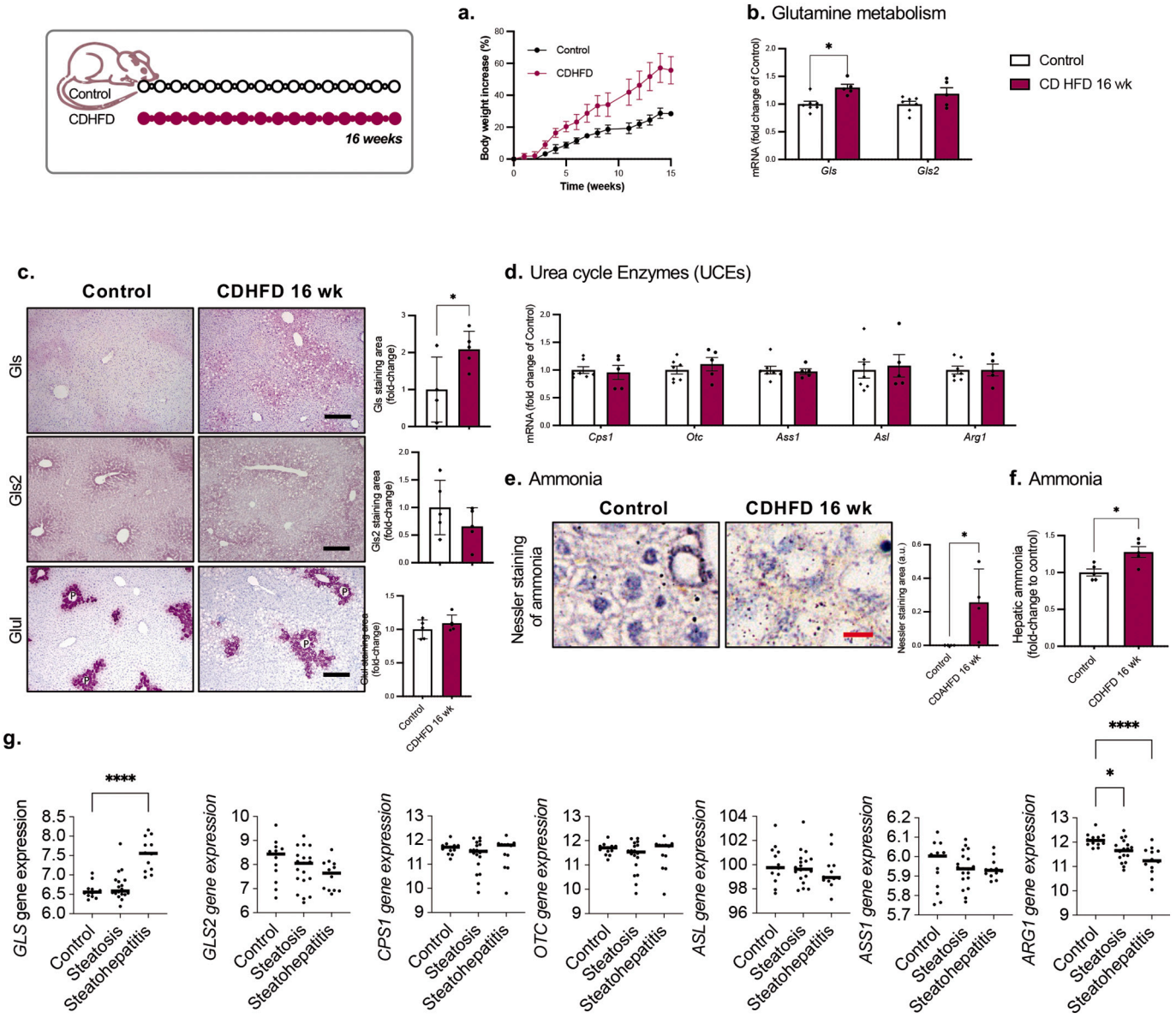

Fig. 4. Disrupted liver nitrogen metabolism in an obesogenic mouse model of diet-induced early steatohepatitis and patients diagnosed with metabolic-associated steatotic liver disease (MASLD). a. Body weight gain, b. Glutamine metabolism mRNA levels, c. Immunohistochemical analysis of hepatic glutamine metabolism enzymes, glutaminase 2 (Gls2), and glutamine synthetase, d. Urea cycle enzymes mRNA levels and hepatic ammonia content measured by e. Nessler histological staining and f. biochemical assay in choline-deficient high-fat diet (CDHFD)-fed rodents for 16 weeks. Data in columns are represented as average ± SEM and a $p < 0.05$ was considered statistically significant after Student's *t*-test comparing with control animals. $^{*}p < 0.05$, and $^{***}p < 0.001$ relative to the control group are shown. At least $n = 5$ rodents were used for each experimental group. Abbreviations: *Glul.* Glutamine synthase, *Gls.* Glutaminase, *Gls2.* Glutaminase 2, *Cps1.* Carbamoyl phosphate synthase 1, *Otc.* Ornithine transcarbamoylase *Ass1.* Arginosuccinate synthetase 1, *Asl.* Arginosuccinate lyase, *Arg1.* Arginase 1. The black scale bar corresponds to 100 mm and the red scale bar to 500 μm. g. Glutamine metabolism and urea cycle genes mRNA expression in patients diagnosed with steatohepatitis versus steatotic patients and healthy control subjects. Data used for this analysis are available and were previously published (Starmann et al., 2012). The data is available in Gene Expression Omnibus (Accession number GSE33814). (For interpretation of the references to colour in this figure legend, the reader is referred to the web version of this article.)

< 0.001) with an increase in plasma ALT (Ctrl = 21 ± 2 vs. AA-diet = 588 ± 201 U/L, $p < 0.05$). Otherwise, treatment with TAK-242 to AA-fed animals reverts the weight loss (AA-diet = 5.3 ± 0.8 vs. AA-diet+TAK-242 = 3.5 ± 0.3 g, $p = 0.07$) and serum ALT levels (AA-diet = 588 ± 201 vs. AA-diet+TAK-242 = 51 ± 18 U/L, $p < 0.05$). The Tlr4 hepatic expression is significantly increased after the AA diet and reduced upon TAK-242 treatment (Fig. 8a). The ACLF animals have been used in a study previously published where BDL/LPS animals are characterized by increased hepatic apoptotic areas and heightened plasma ALT levels, together with augmented expression of hepatic Tlr4. Prophylactic treatment with TAK-242 improves animal survival and reduces apoptotic regions in rat livers normalizing plasma ALT levels. Under these conditions, even though Tlr4 in the liver expression is not significantly altered upon prophylactic TAK-242 treatment cytokines are reduced indicating that Tlr4 signal transduction is impaired [22]. Of relevance, both the AA diet and LPS exposure in BDL rats led to increased hepatic expression of Gls whilst augmenting hepatic ammonia content. In both models, this could be prevented by treatment with the selective Tlr4 inhibitor, TAK-242 (Fig. 8b-d).

Finally, previous reports demonstrated that NF-κB p65 subunit regulates GLS transcription in tumor cells [40–42]. Here, we have confirmed that in CDAHFD-fed rodents for 6 weeks, with augmented

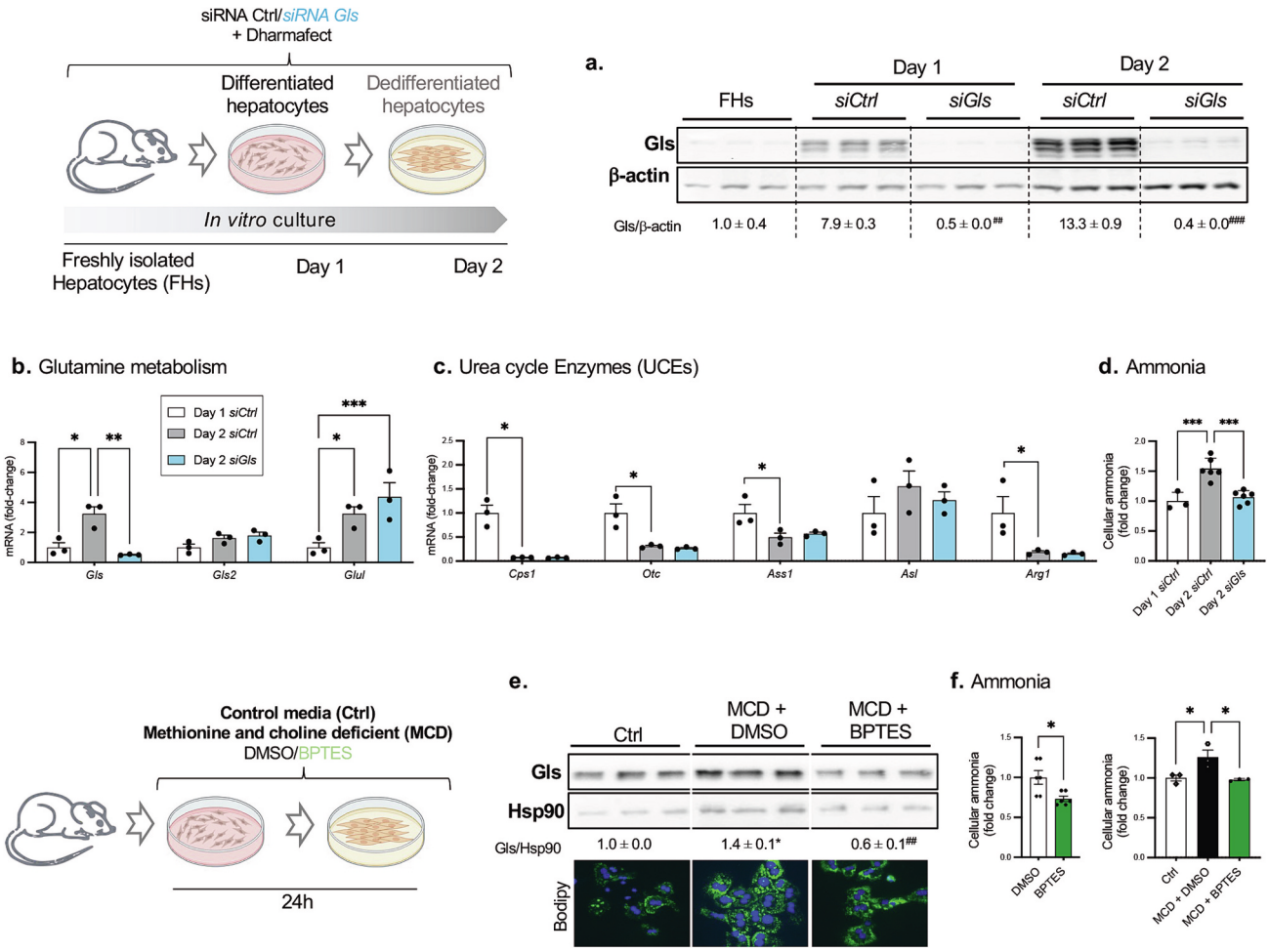

Fig. 5. Specific silencing or pharmacological inhibition of glutaminase 1 (GLS) lowers hepatocyte intracellular ammonia build-up. a. Western blot analysis of Gls expression relative to β-actin; b. Glutamine metabolism genes mRNA levels; c. Urea cycle enzymes mRNA levels, and d. Intracellular ammonia content in isolated primary mouse hepatocytes during their dedifferentiation in culture for 2 days and comparing the effects of Gls silencing (*siGls*) and *siCtrl* by molecular approaches. e. Western blot analysis of Gls expression relative to Hsp90 with bodipy staining of lipids representative immunofluorescence images and f. Intracellular ammonia content in isolated primary mouse hepatocytes after glutaminase 1 pharmacological inhibition with BPTES. Data in columns are represented as average ± SEM and a $p < 0.05$ was considered statistically significant after a one-way ANOVA test and post hoc Tukey's test compared to the control group. *$p < 0.05$, **$p < 0.01$ and ***$p < 0.001$ relative to the control group are shown. At least triplicates were used for each experimental condition. Abbreviations: *Glul*. Glutamine synthase, *Gls*. Glutaminase, *Gls2*. Glutaminase 2, *Cps1*. Carbamoyl phosphate synthase 1, *Otc*. Ornithine transcarbamoylase *Ass1*. Arginosuccinate synthetase 1, *Asl*. Arginosuccinate lyase, *Arg1*. Arginase 1, BPTES. Bis-2-(5-phenylacetamido-1,3,4-thiadiazol-2-yl)ethyl sulfide. Created with BioRender.com.

hepatic GLS expression, the hepatic levels of NF-κB p65 and IKKβ are augmented (Suppl. Fig. 8a). Likewise, well-known targets of NF-κB signaling such as the inflammatory cytokines, *Ccl2* and *Ccl5*, are increased after 6 weeks of CDAHFD (Suppl. Fig. 8b). Moreover, in isolated mouse hepatocytes, the mRNA levels of *Ccl2* and *Ccl5* are increased after stimulation with LPS and reduced upon TAK-242 treatment, further suggesting that NF-κb activation is involved in Gls overexpression.

Overall, our results show that LPS-dependent TLR4 signaling is an upstream regulator of hepatic GLS, in a mechanism related to augmented NF-κb signaling.

4. Discussion

Metabolic-associated steatotic liver disease (MASLD) is the most common chronic liver disease worldwide. Even though Resmetirom has been recently approved as the first drug specific for handling MASLD [43], this condition remains an unmet clinical need that will deeply benefit from a better understanding of its underlying mechanisms and progression hallmarks. On this basis, deregulated ammonia homeostasis has been implicated in MASLD. Indeed, in recent years, several reports have demonstrated a direct relationship between impaired UCEs expression/activity in MASH and the accumulation of hepatic ammonia [10,17,44]. Here, we have confirmed that a compromised urea cycle in mouse models of advanced steatohepatitis is associated with the reprogramming of the hepatic metabolome and accumulation of ornithine and arginine, both urea cycle intermediate metabolites. Ornithine is a substrate for ornithine decarboxylase producing putrescine, a member of the polyamine family, which is increased in steatohepatitis mouse models, whereas hepatic spermine levels, synthesized from putrescine, are not significantly altered. These results agree with earlier findings from other authors, showing that increased polyamine metabolism and rapid export or degradation back to putrescine through polyamine oxidase activity can create high levels of oxidative stress, driving MASH [25]. Also, polyamines are known to be essential for HCC proliferation [45]. In agreement with these findings, increased putrescine in association with the presence of proliferative markers, such as Ki67 was observed in rodents fed a CDAHFD-fed for 6 weeks, a dietary mouse model that develops MASH-related liver cancer [24,46].

Hepatic ammonia is also a by-product of glutaminase metabolism. Our group and others have previously shown that the hepatic high-activity GLS isoform is overexpressed in the livers of pre-clinical

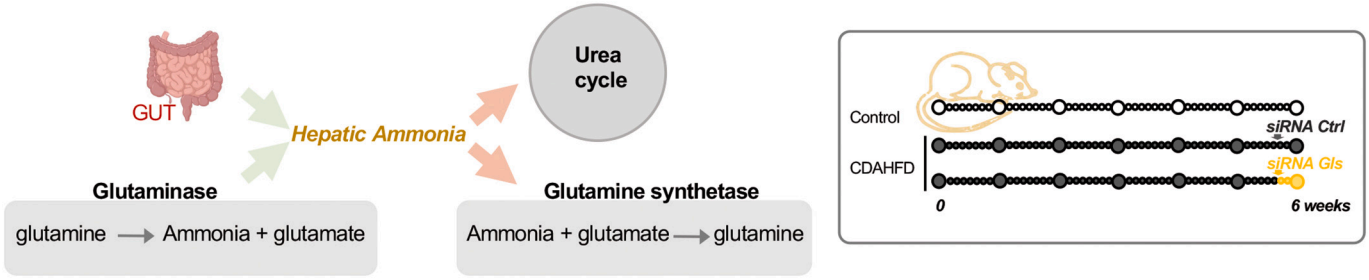

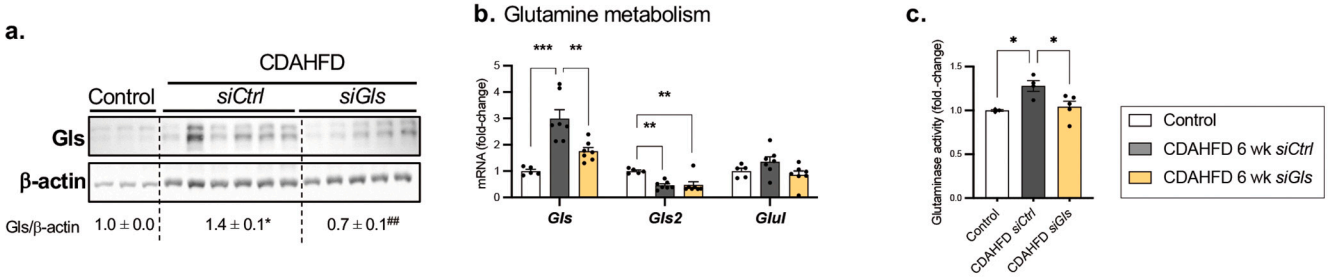

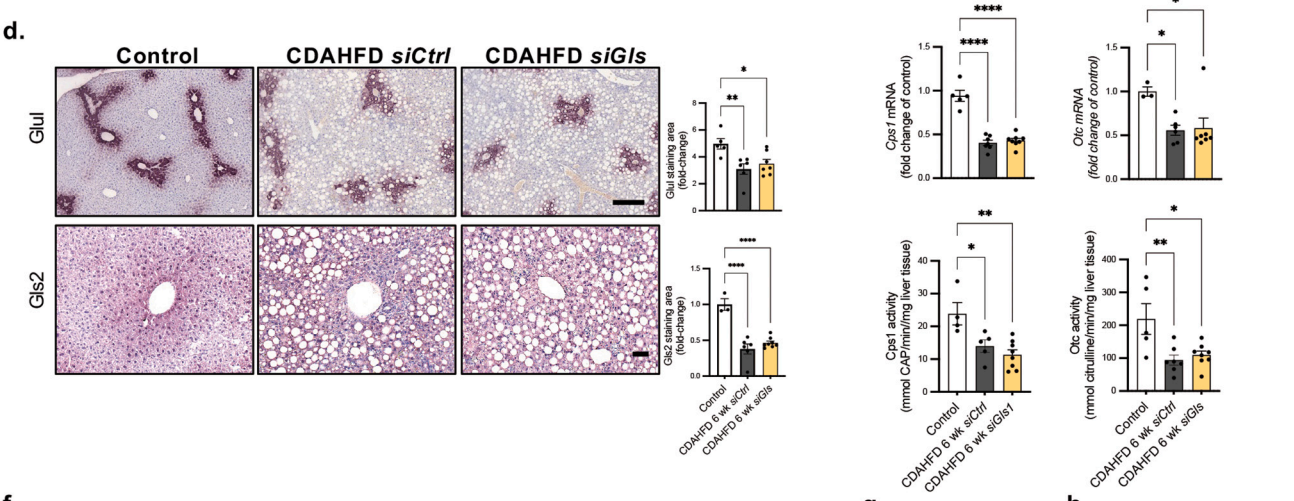

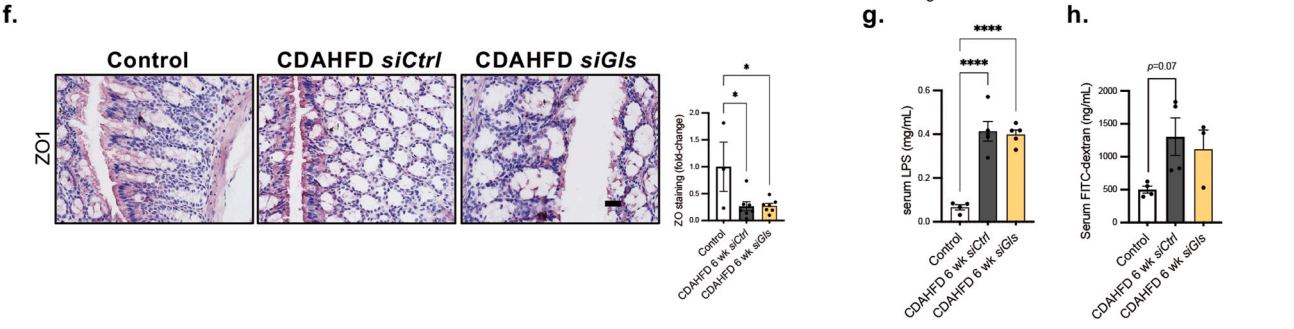

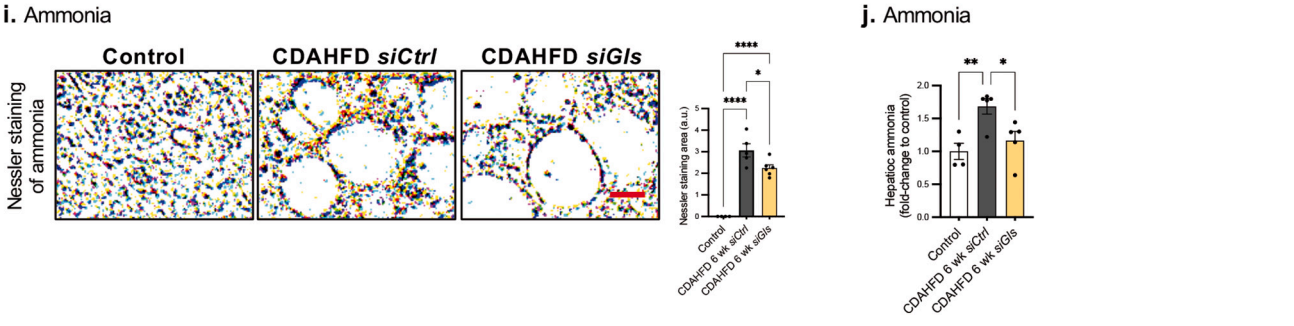

(caption on next page)

Fig. 6. Acute silencing of hepatic glutaminase 1 (GLS) diminishes hepatic ammonia build-up in a pre-clinical mouse model of diet-induced steatohepatitis. a. Western blot analysis of Gls expression relative to β-actin; b. Glutamine metabolism genes mRNA levels; c. Liver glutaminase activity; d. Immunohistochemical analysis of hepatic glutamine metabolism enzymes, Gls2 and Glul; e. Urea cycle enzymes, Cps1 and Otc, hepatic mRNA levels and activity; f. Immunohistochemical analysis of intestine zonula occludens-1 (ZO1) staining; g. Serum LPS levels; h. Serum FITC-dextran levels; and Hepatic ammonia content measured by i. Nessler staining histological analysis and j. biochemical assay in choline deficient L-amino acid-defined high fat diet (CDAHFD)-fed rodents for 6 weeks and after acute silencing of hepatic Gls by intravenous injection using siRNA against Gls (*siGls*) or untargeted scrambled control siRNA (*siCtrl*). Data in columns are represented as average ± SEM. A $p < 0.05$ was considered statistically significant after a one-way ANOVA and post-hoc Tukey's tests compared to the control group. *$p < 0.05$, **$p < 0.01$ and ****$p < 0.0001$ relative to the control group are shown. At least $n = 5$ rodents were used for each experimental group. Abbreviations: *Glul.* Glutamine synthase, *Gls.* Glutaminase, *Gls2.* Glutaminase 2, *Cps1.* Carbamoyl phosphate synthase 1, *Otc.* Ornithine transcarbamoylase. The black scale bar corresponds to 100 μm and the red scale bar to 500 μm. (For interpretation of the references to colour in this figure legend, the reader is referred to the web version of this article.) Created with BioRender.com.

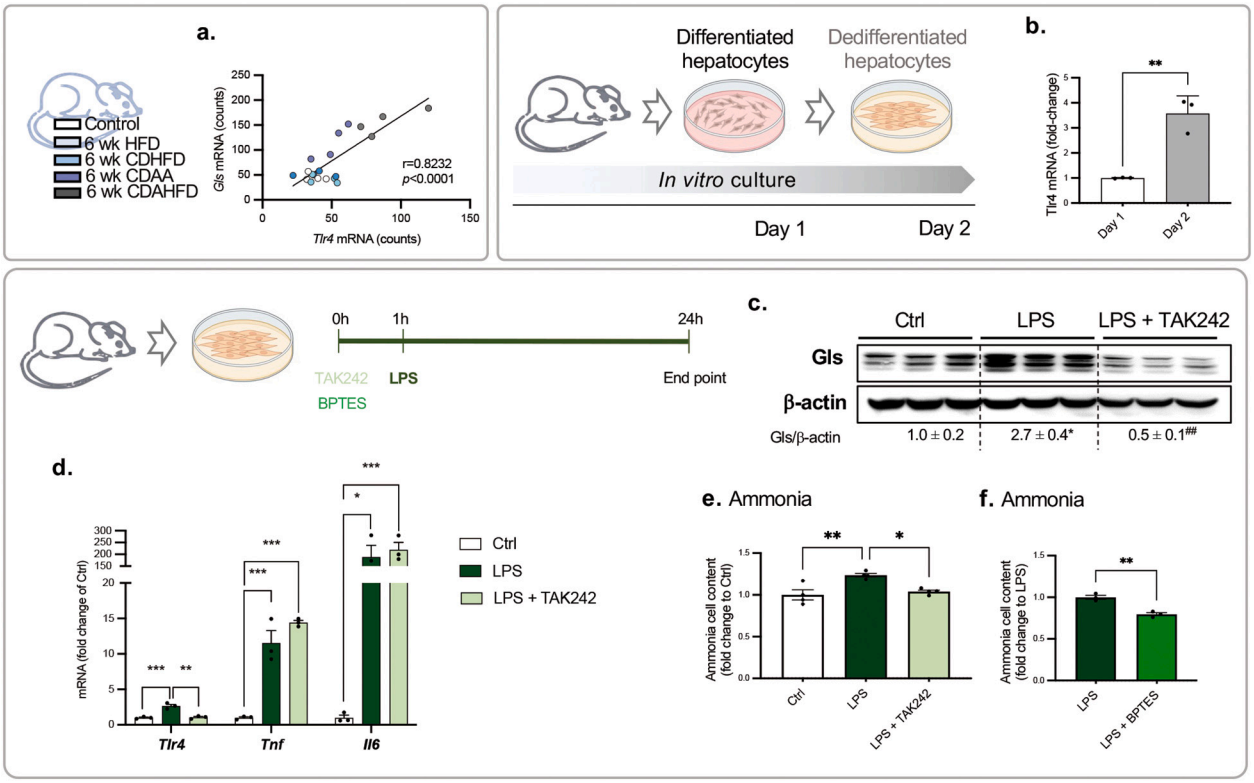

Fig. 7. Toll-like receptor 4 (TLR4) is an upstream regulator of hepatic glutaminase 1 (GLS). a. Pearson correlations between transcriptional expression of hepatic glutaminase 1 (*Gls*) and toll-like receptor 4 (*Tlr4*) in animal models of diet-induced MASLD. Mice were maintained for 6 weeks on a high-fat diet (HFD), choline-deficient high-fat diet (CDHFD), choline-deficient L-amino acid-defined diet (CDAA), and choline-deficient L-amino acid-defined high-fat diet (CDAHFD) and compared to standard rodent chow diet (Control). Pearson coefficient (r) and *p*-value are shown in the graph. b. *Tlr4* mRNA expression in isolated primary mouse hepatocytes during their dedifferentiation in culture for 2 days. c. Western blot analysis of Gls expression relative to β-actin, d. mRNA levels of hepatocyte *Tlr4*, *Tnf* and *Il6*; and e. Intracellular ammonia content in isolated primary mouse hepatocytes after exposure to lipopolysaccharide (LPS) in the presence and absence of the Tlr4 pharmacological inhibitor, TAK242. f. Intracellular ammonia content in isolated primary mouse hepatocytes after exposure to LPS in the presence and absence of the Gls pharmacological inhibitor, BPTES. Data in columns are represented as average ± SEM. A $p < 0.05$ was considered statistically significant after a one-way ANOVA and post-hoc Tukey's tests compared to the control group. *$p < 0.05$, **$p < 0.01$ and ****$p < 0.0001$ relative to the respective control group are shown. At least $n = 4$ rodents were used for each experimental group and triplicate experiments were performed for the cell-based studies. Abbreviations: Tnf. Tumor necrosis factor, Il6. Interleukin 6. BPTES. Bis-2-(5-phenylacetamido-1,3,4-thiadiazol-2-yl)ethyl sulfide. Created with BioRender.com.

models and clinical biopsies of MASH and liver fibrosis [14,15,28]. In agreement with these findings, we have found that the high-activity GLS isoform is transcriptionally upregulated in liver biopsies of MASH mouse models in comparison with healthy controls and animals with simple steatosis. More specifically, a glutaminase isoform metabolic switch occurs with reduced expression of GLS2 and increased GLS, in many ways mimicking what is observed in liver cancer [47–49]. In agreement with this, we have observed that hepatocytes that undergo a dedifferentiation process in culture also undergo a similar glutaminase isoform switch. Whereas in healthy livers, liver glutamine metabolized by GLS2 is used mostly as a substrate for gluconeogenesis and urea synthesis, the GLS isoform in the fetal liver utilizes glutamine for biosynthetic purposes and possibly as a respiratory fuel [50,51]. In addition, whereas ammonia synthesized by GLS2, co-localized in the periportal region together with the UCEs, is used as an amplification system to boost ureagenesis and eliminate this excess ammonia [52], ammonia synthesized by GLS, which has a wider distribution throughout the liver parenchyma, can have a more substantial negative impact in hepatic ammonia accumulation. Importantly, we have found that overexpression of hepatic GLS is an early event in the accumulation of hepatic ammonia underlying steatohepatitis, preceding the observed changes in UCEs in the dietary MASLD animal models studied. These findings are also found in the clinical setting when comparing patients with steatohepatitis with patients with steatosis and control subjects, augmented hepatic expression of GLS is observed whereas mRNA levels of the majority of UCEs remain unaltered [29]. Significantly, we have

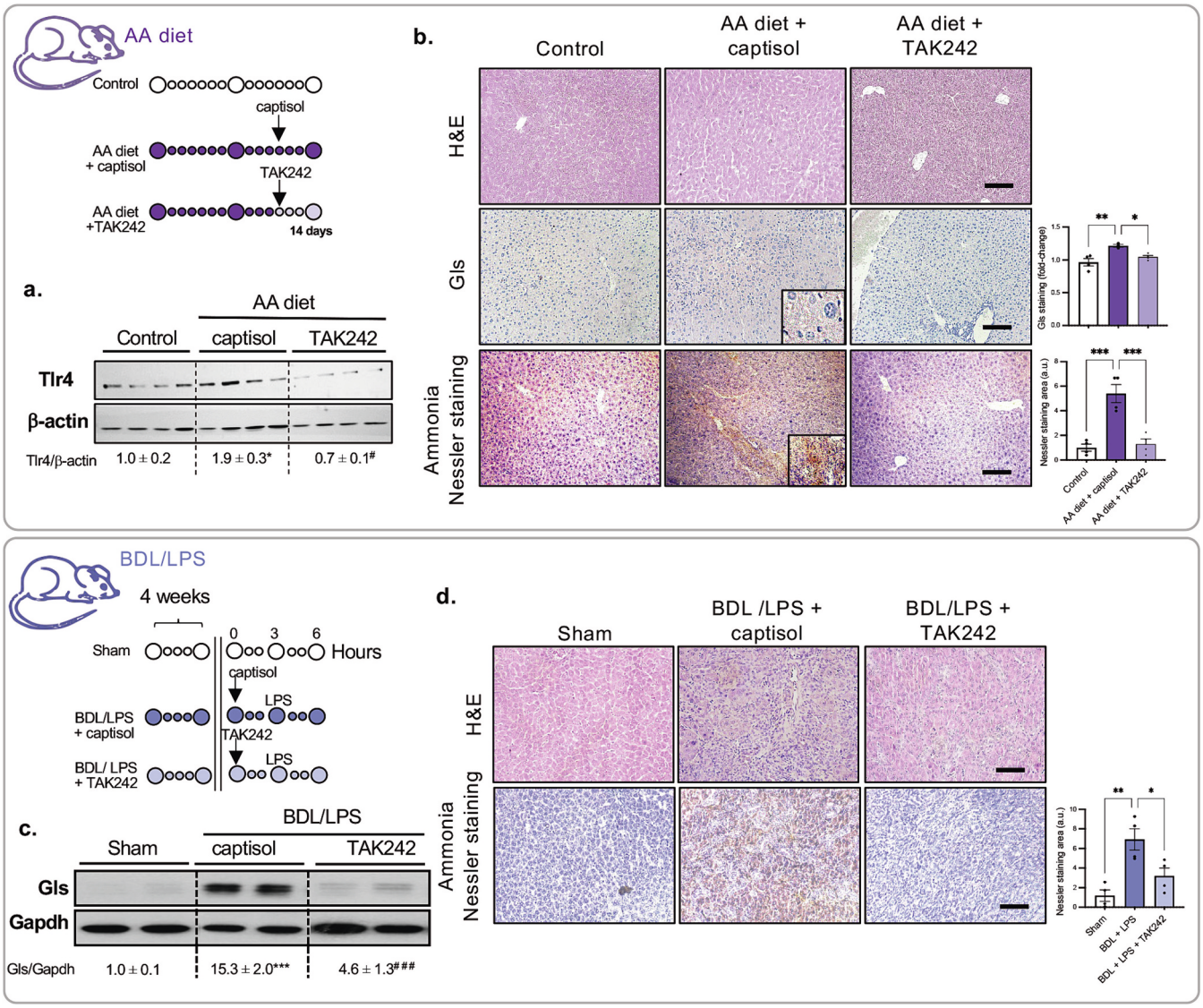

Fig. 8. Effect of Toll-like receptor 4 (Tlr4) pharmacological inhibition in hepatic glutaminase 1 (GLS) level in animal models of hyperammonemia and endotoxemia. a. Western blot analysis of Tlr4 expression relative to β-actin and b. Hematoxylin and Eosin (H&E) and immunohistochemical analysis of hepatic Gls and liver Nessler staining of ammonia in mice fed with an amino acid-enriched diet (AA diet) for 14 days and treated with TAK242 at 4 days before end point. c. Western blot analysis of Gls expression relative to Gapdh and d. Immunohistochemical analysis of liver Nessler staining of ammonia in bile-duct ligated rats exposed to LPS and prophylactically treated with TAK242. Data in columns are represented as average ± SEM. A $p < 0.05$ was considered statistically significant after a one-way ANOVA and post-hoc Tukey's tests compared to the control group. *$p < 0.05$, **$p < 0.01$ and ****$p < 0.0001$ relative to the respective control group are shown. At least n = 4 rodents were used for each experimental group. The black scale bar corresponds to 100 μm.

also shown that the specific silencing or pharmacological inhibition of hepatic GLS, both in an in vitro model of dedifferentiated hepatocytes and a mouse model of advanced steatohepatitis, reduces hepatic ammonia content without concomitant changes in UCEs, glutamine synthetase or gut integrity and endotoxemia, other key intermediates involved in liver ammonia homeostasis. Even though our findings highlight the important role played by augmented hepatic GLS in controlling hepatic hyperammonemia underlying experimental MASH, it is important to further validate our findings in liver specimens of patients with steatohepatitis or human hepatocytes as the pre-clinical dietary models used do not always replicate human MASH. Indeed, most of the dietary animal models of MASLD used here are not characterized by obesity and insulin resistance, two hallmarks of human pathology.

The mechanisms underlying GLS upregulation underlying steatohepatitis were further explored here. Previous results have described that in some types of cancers including hepatocellular carcinoma GLS is epigenetically regulated by its promoter hypomethylation. Thus, we initially evaluated the GLS promoter methylation state in mouse liver biopsies of animal models of MASLD. Only advanced mouse models of steatohepatitis present a significant downregulation of GLS promoter methylation, suggesting that other mechanisms underlie the initial GLS upregulation in MASH. Metabolic endotoxemia, the chronic elevation of serum LPS levels, is a hallmark of MASH [37,38] and LPS acts on cells mainly through the actions of its receptor, TLR4 [53]. According to our multiplex transcriptomic analysis of the different animal models of diet-induced MASLD, gene sets related to TLR signaling are strongly associated with the onset of steatohepatitis. Indeed, we showed that hepatic GLS overexpression shows a strong positive correlation with liver TLR4 expression in mouse models of diet-induced MASLD and is also increased in dedifferentiated hepatocytes with elevated GLS expression. Conversely, *Tlr4*$^{-/-}$ mice present reduced liver GLS expression in association with reduced hepatic ammonia accumulation.

Early reports identified the presence of TLR receptors on liver monocytes, macrophages, Kupffer cells, and dendritic cells [54].

However, other posterior studies have shown that hepatocytes express the TLR4 protein on the cell surface [55] and can directly respond to LPS without the mediation of Kupffer cells and macrophages [55], suggesting that this LPS-mediated hepatocyte activation could be implicated in the pathogenesis of endotoxin-induced liver injury. As both TLR4 signaling and GLS hepatic expression are closely related to the onset of steatohepatitis we hypothesized that TLR4 is an upstream regulator of GLS in the hepatocyte. Here, we found that stimulation of isolated primary mouse hepatocytes with LPS induces GLS expression, a process hampered by the specific pharmacological inhibition of TLR4.

Consistent with these results, hepatic GLS expression is heightened in animal models of endotoxemia where pre-treatment with the pharmacological inhibitor of TLR4 halts hepatic GLS expression. Importantly, hepatic GLS expression under these conditions results in augmented hepatic ammonia concentrations. These results agree with earlier works showing that glutaminolysis is increased in intact mitochondria from endotoxin-injected mice [56]. Also, earlier investigations on an *in vitro* neuroinflammation model revealed that GLS is increased in primary mouse microglia following pro-inflammatory stimulus whereas treatment with the GLS-specific inhibitor, BPTES, reversed LPS-induced microglial activation and inflammation [57]. Notably, LPS can potentially affect ammonia metabolism independently of GLS. On this basis, Soria *et al.* have shown that LPS impairs hepatocyte ureagenesis from ammonia by inhibiting hepatocyte mitochondrial aquaporin-8 (mtAQP8) in the inner mitochondrial membranes and therefore halting the diffusional transport of ammonia [58].

Finally, it has been demonstrated that on the one hand, LPS leads to the rapid degradation of IκB-α activating NF-κB-dependent transcription [55]. On the other hand, it has been shown that NF-κB p65 regulates the expression and activity of GLS in human cancer cells by different mechanisms which include an indirect effect through c-myc and mir-23a [40], the epidermal growth factor receptor 2 (ErbB2) [42] or a direct effect on the GLS promoter [41]. Our findings also indicate the close relationship between the LPS/TLR4 axis and NF-κB signaling underlying GLS upregulation in steatohepatitis by mechanisms that need to be further studied.

Overall, our results suggest that metabolic endotoxemia during MASH triggers TLR4 hepatic signaling, inducing GLS overexpression. In early steatohepatitis, increased hepatic GLS drives the accumulation of hepatic ammonia, preceding the reduced expression of UCEs. Hypothetically, this initial accumulation of GLS-generated ammonia, a metabolite previously associated with changes in methylation patterns of some genes in plants [59], may further alter the methylation of the promoters of the UCEs and GLS and GLS2 causing their downregulation, as described in mouse models and clinical biopsies of patients with MASH [10,44]. Upon decreased expression of the UCEs and glutamine synthetase, hepatic ammonia is further increased eventually leading to systemic hyperammonemia. Excessive ammonia in the serum is a pathogenic factor potentially accounting for MASLD-related multiorgan dysfunction and disease progression [60]. In summary, we have demonstrated that hepatic GLS overexpression has a causal role in the accumulation of hepatic ammonia underlying steatohepatitis and that the specific silencing of hepatic GLS, either by using pharmacological inhibitors or molecular approaches, is an effective therapeutic strategy for scavenging hepatic ammonia.

CRediT authorship contribution statement

Maria Mercado-Gómez: Writing – original draft, Methodology, Conceptualization. **Naroa Goikoetxea-Usandizaga:** Methodology, Investigation. **Annarein J.C. Kerbert:** Methodology, Investigation. **Leire Uraga Gracianteparaluceta:** Methodology, Investigation. **Marina Serrano-Maciá:** Methodology, Investigation. **Sofia Lachiondo-Ortega:** Methodology, Investigation. **Rubén Rodriguez-Agudo:** Methodology, Investigation. **Clàudia Gil-Pitarch:** Methodology, Investigation. **Jorge Simón:** Methodology, Investigation. **Irene González-Recio:** Methodology, Investigation. **Marcos F. Fondevila:** Investigation, Funding acquisition. **Pablo Santamarina-Ojeda:** Methodology, Investigation. **Mario F. Fraga:** Methodology, Investigation. **Rubén Nogueiras:** Writing – review & editing, Conceptualization. **Javier de las Heras:** Writing – review & editing, Conceptualization. **Rajiv Jalan:** Writing – review & editing, Conceptualization. **María Luz Martínez-Chantar:** Writing – original draft, Conceptualization. **Teresa C. Delgado:** Writing – original draft, Methodology, Investigation, Conceptualization.

Declaration of competing interest

The authors have declared that no conflict of interest exists.

Acknowledgements

TC Delgado is funded by “Ayuda RYC2020-029316-I financiada por MCIN/AEI/10.13039/501100011033 y por El FSE invierte en tu future”. This work was supported by the Gilead Sciences Research Scholars Program in Global Liver (to TCD), Nanostring® grant (to TCD); grant from Ministerio de Ciencia, Innovación y Universidades (MICINN: PID2022-139395OB-100 integrado en el Plan Estatal de Investigación Científica y Técnica e Innovación, con Fondos FEDER); grants from Ministerio de Ciencia, Innovación y Universidades MICINN: PID2020-117116RB-I00 CEX2021-001136-S integrado en el Plan Estatal de Investigación Científica y Técnica e Innovación, cofinanciado con Fondos FEDER for (MLM-C); Project funded by CIBEREHD; La Caixa Scientific Foundation (HR17-00601) (for MLM-C); ERA-Net E-Rare EJP RD Joint Translational Call for Rare Diseases FIGHT-CNNM2 (EJPRD19-040), and from Instituto Carlos III, Spain (for MLM-C, JH); the Basque Department of Education (IT1739-22) (for JH). JH and TCD are members of the European Reference Network for Rare Hereditary Metabolic Disorders (MetabERN) Project ID No. 739543.

Appendix A. Supplementary data

Supplementary data to this article can be found online at https://doi.org/10.1016/j.metabol.2024.155952.

References

[1] Gebhardt R, Matz-Soja M. Liver zonation: novel aspects of its regulation and its impact on homeostasis. World J Gastroenterol 2014;20(26):8491–504.
[2] Jungermann K, Kietzmann T. Zonation of parenchymal and nonparenchymal metabolism in liver. Annu Rev Nutr 1996;16:179–203.
[3] Wang P, et al. Gut microbiome-derived ammonia modulates stress vulnerability in the host. Nat Metab 2023;5:1986–2001.
[4] Kotsiliti E. Hyperammonaemia in liver cirrhosis. Nat Rev Gastroenterol Hepatol 2022;19(10):624.
[5] Mathias RS, Kostiner D, Packman S. Hyperammonemia in urea cycle disorders: role of the nephrologist. Am J Kidney Dis 2001;37(5):1069–80.
[6] Jalan R, Lee WM. Treatment of hyperammonemia in liver failure: a tale of two enzymes. Gastroenterology 2009;136(7):2048–51.
[7] Jover-Cobos M, Khetan V, Jalan R. Treatment of hyperammonemia in liver failure. Curr Opin Clin Nutr Metab Care 2014;17(1):105–10.
[8] Adeva MM, et al. Ammonium metabolism in humans. Metabolism 2012;61(11):1495–511.
[9] Gutierrez-de-Juan V, et al. A morphological method for ammonia detection in liver. PLoS One 2017;12(3):e0173914.
[10] De Chiara F, et al. Urea cycle dysregulation in non-alcoholic fatty liver disease. J Hepatol 2018;69(4):905–15.
[11] Song Q, et al. Gut-derived ammonia contributes to alcohol-related fatty liver development via facilitating ethanol metabolism and provoking ATF4-dependent de novo lipogenesis activation. Metabolism 2024;151:155740.
[12] Aron-Wisnewsky J, et al. Gut microbiota and human NAFLD: disentangling microbial signatures from metabolic disorders. Nat Rev Gastroenterol Hepatol 2020;17(5):279–97.
[13] Loomba R, et al. Gut microbiome-based metagenomic signature for non-invasive detection of advanced fibrosis in human nonalcoholic fatty liver disease. Cell Metab 2017;25(5). p. 1054-1062 e5.
[14] Simon J, et al. Targeting hepatic glutaminase 1 ameliorates non-alcoholic steatohepatitis by restoring very-low-density lipoprotein triglyceride assembly. Cell Metab 2020;31(3). p. 605-622 e10.

[15] Du K, et al. Hedgehog-YAP signaling pathway regulates Glutaminolysis to control activation of hepatic stellate cells. Gastroenterology 2018;154(5). p. 1465-1479 e13.
[16] Thomsen KL, et al. Ammonia: a novel target for the treatment of non-alcoholic steatohepatitis. Med Hypotheses 2018;113:91–7.
[17] De Chiara F, et al. Ammonia scavenging prevents progression of fibrosis in experimental nonalcoholic fatty liver disease. Hepatology 2020;71(3):874–92.
[18] Canbay A, et al. l-Ornithine-l-Aspartate (LOLA) normalizes metabolic parameters in models of steatosis, insulin resistance and metabolic syndrome. Pharmaceutics 2024;16(4).
[19] Tu H, et al. Glutaminase 1 blockade alleviates nonalcoholic steatohepatitis via promoting proline metabolism. Biochem Biophys Res Commun 2022;634:1–9.
[20] Balata S, et al. Induced hyperammonemia alters neuropsychology, brain MR spectroscopy and magnetization transfer in cirrhosis. Hepatology 2003;37(4): 931–9.
[21] Olde Damink SW, et al. Upper gastrointestinal bleeding: an ammoniagenic and catabolic event due to the total absence of isoleucine in the haemoglobin molecule. Med Hypotheses 1999;52(6):515–9.
[22] Engelmann C, et al. Toll-like receptor 4 is a therapeutic target for prevention and treatment of liver failure. J Hepatol 2020;73(1):102–12.
[23] Liang W, et al. Establishment of a general NAFLD scoring system for rodent models and comparison to human liver pathology. PLoS One 2014;9(12):e115922.
[24] Matsumoto M, et al. An improved mouse model that rapidly develops fibrosis in non-alcoholic steatohepatitis. Int J Exp Pathol 2013;94(2):93–103.
[25] Quinn C, et al. Dysregulation of S-adenosylmethionine metabolism in nonalcoholic steatohepatitis leads to polyamine flux and oxidative stress. Int J Mol Sci 2022;23 (4).
[26] Iruarrizaga-Lejarreta M, et al. Role of Aramchol in steatohepatitis and fibrosis in mice. Hepatol Commun 2017;1(9):911–27.
[27] Sookoian S, et al. Nonalcoholic steatohepatitis is associated with a state of betaine-insufficiency. Liver Int 2017;37(4):611–9.
[28] Du K, et al. Increased glutaminolysis marks active scarring in nonalcoholic steatohepatitis progression. Cell Mol Gastroenterol Hepatol 2020;10(1):1–21.
[29] Starmann J, et al. Gene expression profiling unravels cancer-related hepatic molecular signatures in steatohepatitis but not in steatosis. PLoS One 2012;7(10): e46584.
[30] Mizuguchi T, et al. Alteration of expression of liver-enriched transcription factors in the transition between growth and differentiation of primary cultured rat hepatocytes. J Cell Physiol 1998;174(3):273–84.
[31] Vachher M, et al. Deciphering the role of aberrant DNA methylation in NAFLD and NASH. Heliyon 2022;8(10):e11119.
[32] Takumi S, et al. The effect of a methyl-deficient diet on the global DNA methylation and the DNA methylation regulatory pathways. J Appl Toxicol 2015;35(12): 1550–6.
[33] D'Aquila P, et al. Gut microbiota as important mediator between diet and DNA methylation and histone modifications in the host. Nutrients 2020;12(3).
[34] Jones PA. Functions of DNA methylation: islands, start sites, gene bodies and beyond. Nat Rev Genet 2012;13(7):484–92.
[35] Chandrashekar DS, et al. UALCAN: a portal for facilitating tumor subgroup gene expression and survival analyses. Neoplasia 2017;19(8):649–58.
[36] Chandrashekar DS, et al. UALCAN: an update to the integrated cancer data analysis platform. Neoplasia 2022;25:18–27.
[37] Luther J, et al. Hepatic injury in nonalcoholic steatohepatitis contributes to altered intestinal permeability. Cell Mol Gastroenterol Hepatol 2015;1(2):222–32.
[38] Kessoku T, et al. Endotoxins and non-alcoholic fatty liver disease. Front Endocrinol (Lausanne) 2021;12:770986.
[39] Sharifnia T, et al. Hepatic TLR4 signaling in obese NAFLD. Am J Physiol Gastrointest Liver Physiol 2015;309(4):G270–8.
[40] Rathore MG, et al. The NF-kappaB member p65 controls glutamine metabolism through miR-23a. Int J Biochem Cell Biol 2012;44(9):1448–56.
[41] Dong M, et al. Nuclear factor-kappaB p65 regulates glutaminase 1 expression in human hepatocellular carcinoma. Onco Targets Ther 2018;11:3721–9.
[42] Qie S, et al. ErbB2 activation upregulates glutaminase 1 expression which promotes breast cancer cell proliferation. J Cell Biochem 2014;115(3):498–509.
[43] Kokkorakis M, et al. Resmetirom, the first approved drug for the management of metabolic dysfunction-associated steatohepatitis: trials, opportunities, and challenges. Metabolism 2024;154:155835.
[44] Gallego-Duran R, et al. Liver injury in non-alcoholic fatty liver disease is associated with urea cycle enzyme dysregulation. Sci Rep 2022;12(1):3418.
[45] Novita Sari I, et al. Metabolism and function of polyamines in cancer progression. Cancer Lett 2021;519:91–104.
[46] Wei G, et al. Comparison of murine steatohepatitis models identifies a dietary intervention with robust fibrosis, ductular reaction, and rapid progression to cirrhosis and cancer. Am J Physiol Gastrointest Liver Physiol 2020;318(1): G174–88.
[47] Katt WP, Lukey MJ, Cerione RA. A tale of two glutaminases: homologous enzymes with distinct roles in tumorigenesis. Future Med Chem 2017;9(2):223–43.
[48] Wang JB, et al. Targeting mitochondrial glutaminase activity inhibits oncogenic transformation. Cancer Cell 2010;18(3):207–19.
[49] Hu W, et al. Glutaminase 2, a novel p53 target gene regulating energy metabolism and antioxidant function. Proc Natl Acad Sci USA 2010;107(16):7455–60.
[50] Mates JM, et al. Glutaminase isoenzymes as key regulators in metabolic and oxidative stress against cancer. Curr Mol Med 2013;13(4):514–34.
[51] Elgadi KM, et al. Cloning and analysis of unique human glutaminase isoforms generated by tissue-specific alternative splicing. Physiol Genomics 1999;1(2): 51–62.
[52] Haussinger D. Liver glutamine metabolism. JPEN J Parenter Enteral Nutr 1990;14 (4 Suppl):56S–62S.
[53] Beutler B. Tlr4: central component of the sole mammalian LPS sensor. Curr Opin Immunol 2000;12(1):20–6.
[54] Su GL, et al. Kupffer cell activation by lipopolysaccharide in rats: role for lipopolysaccharide binding protein and toll-like receptor 4. Hepatology 2000;31 (4):932–6.
[55] Migita K, et al. Lipopolysaccharide signaling induces serum amyloid A (SAA) synthesis in human hepatocytes in vitro. FEBS Lett 2004;569(1–3):235–9.
[56] Ewart HS, Qian D, Brosnan JT. Activation of hepatic glutaminase in the endotoxin-treated rat. J Surg Res 1995;59(2):245–9.
[57] Gao G, et al. Glutaminase C regulates microglial activation and pro-inflammatory exosome release: relevance to the pathogenesis of Alzheimer's disease. Front Cell Neurosci 2019;13:264.
[58] Soria LR, et al. Lipopolysaccharide impairs hepatocyte ureagenesis from ammonia: involvement of mitochondrial aquaporin-8. FEBS Lett 2014;588(9):1686–91.
[59] Kim JY, et al. Ammonium inhibits chromomethylase 3-mediated methylation of the Arabidopsis nitrate reductase gene NIA2. Front Plant Sci 2015;6:1161.
[60] Thomsen KL, et al. Role of ammonia in NAFLD: an unusual suspect. JHEP Rep; 2023.